



13TH CANADIAN MASONRY SYMPOSIUM
HALIFAX, CANADA
JUNE 4TH – JUNE 7TH 2017



BEHAVIOUR OF MASONRY WALLS AT CORNERS UNDER LATERAL LOADS

Bansal, Nitin¹ and Rai, Durgesh.C.²

ABSTRACT

Majority of the masonry research work deals with its failure due to either in-plane (IP) or out-of-plane (OP) lateral forces. However, failure of masonry walls at corners, though frequent, has not been researched much. Such failure involves the detachment of a wedge shaped portion of masonry from the corner walls under the action of bidirectional lateral load. Behaviour of corners in dry stack masonry was studied up to failure in ABAQUS, Finite Element (FE) environment using explicit solver. Various models of masonry structures with loadbearing and non-loadbearing walls were considered and were subjected to dynamic loading along the corner. Based on the failure pattern observed under the simultaneous action of IP and OP forces, simplified corner failure mechanisms were proposed for the limiting equilibrium condition and corresponding values of peak acceleration were obtained. Results of limit analysis compared well with FE predictions. The FE approach adopted for dry stack masonry was extended to study the corner failure in mortar bonded masonry. A distinct friction coefficient for each course was introduced which was equivalent to the shear resisted by the layer of mortar in any given course. Such a method of modelling was effective in determining the propagation of cracks through the masonry as well as the value of acceleration at which a portion of corner wall detaches from the rest of the masonry. This study not only helped in understanding the failure pattern of corner masonry walls, but also provided an approach to estimate the limit strength in terms of peak acceleration.

KEYWORDS: *corner failure, dry masonry, mortar bonded masonry, finite element, distinct friction coefficient*

INTRODUCTION

Masonry structures which either stand isolated or located at the end of a row of structures often experience damage at corners in earthquakes as shown in Figure 1. Such damages are generally characterized by simultaneous detachment of a portion of orthogonal walls. The shape of this

¹ Frm. Graduate Student, Department of Civil Engineering, Indian Institute of Technology Kanpur, Kanpur, Uttar Pradesh, India, nitinbansal64@gmail.com

² Professor, Department of Civil Engineering, Indian Institute of Technology Kanpur, Kanpur, Uttar Pradesh, India, dcrai@iitk.ac.in

detached portion of masonry is like that of a wedge with its apex pointing downwards and overturning about it. A method proposed earlier to calculate the limiting load for such a failure in dry stack masonry had certain limitations which are addressed in this study [4].

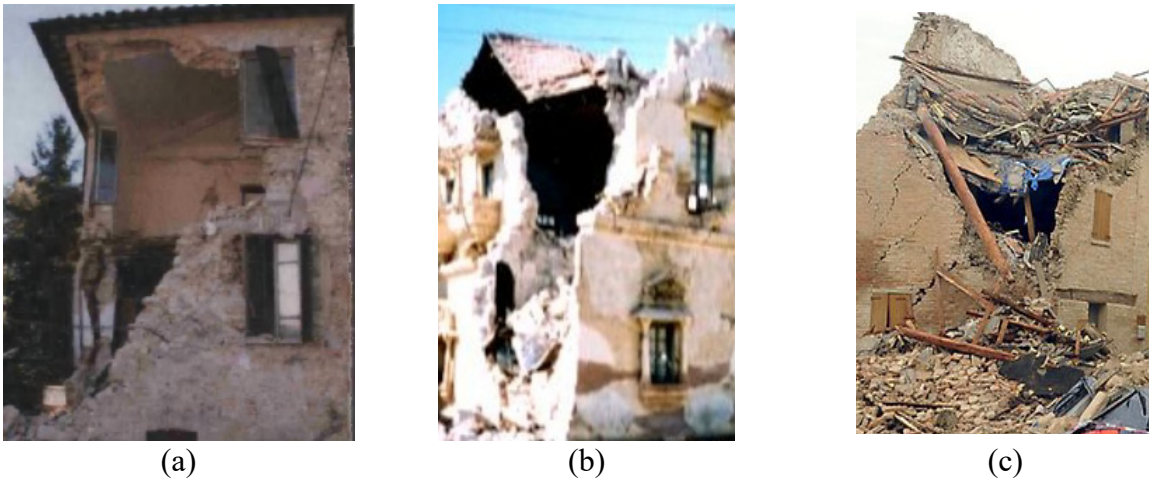


Figure 1: Corner failure in masonry structure a) 1999, Umbria Earthquake [1] b) 2001 Gujarat Earthquake [2] and c) 2009 L'Aquila Earthquake [3]

The main objectives of this study are: to develop a better understanding about the formation of mechanism for masonry corner failures under earthquakes and to provide estimates of the corresponding limiting acceleration. Such types of failures are observed both in dry-stack masonry as well as mortar-bonded masonry. Therefore, behaviour of both types of masonry was investigated using ABAQUS Finite Element (FE) environment. Such failure is generally expected to occur when the lateral load or its resultant acts along the corner as shown in Figure 2(a). However, the angle at which the lateral load acts on the structure varies from one earthquake to another earthquake. Therefore, for this study, accelerating motion has been assumed to act diagonally along the corner making angles θ_s and θ_f with the side wall and the façade respectively as shown in Figure 2(b) and 2(c).

FINITE ELEMENT MODELLING

In order to model the masonry structure, brick units were modelled separately and stacked to form the masonry walls. Concrete damage plasticity (CDP) model of ABAQUS, which is suitable for modelling concrete like materials, was adopted to model the brick masonry. A simple tri-linear stress strain curve for masonry in compression was used [5]. Peak tensile strength of masonry was considered 10 percent of its compressive strength [6]. These assumed stress strain curves for masonry in compression and tension are shown in Figure 3. Keeping in mind the experimental facilities available at the Structural Engineering Laboratory at IIT Kanpur, half-scaled bricks of size $120 \times 60 \times 37.5$ mm are used for the physical test models and the same was adopted for the FE modelling so that results can be directly correlated with experiments. Structurally ineffective masses (artificial masses) need to be added to reduced-scaled models for proper simulation of both gravitational and inertial forces [7]. For out-of-plane ground motions

of masonry wall panels, the artificial mass should also be distributed throughout the wall so that resulting inertia forces are uniformly distributed. The artificial mass that needs to be added for unit acceleration ratio in half-scale models, is equal to the mass of a half-scaled brick, which can be simulated in FE model by doubling the density of brick material [8].

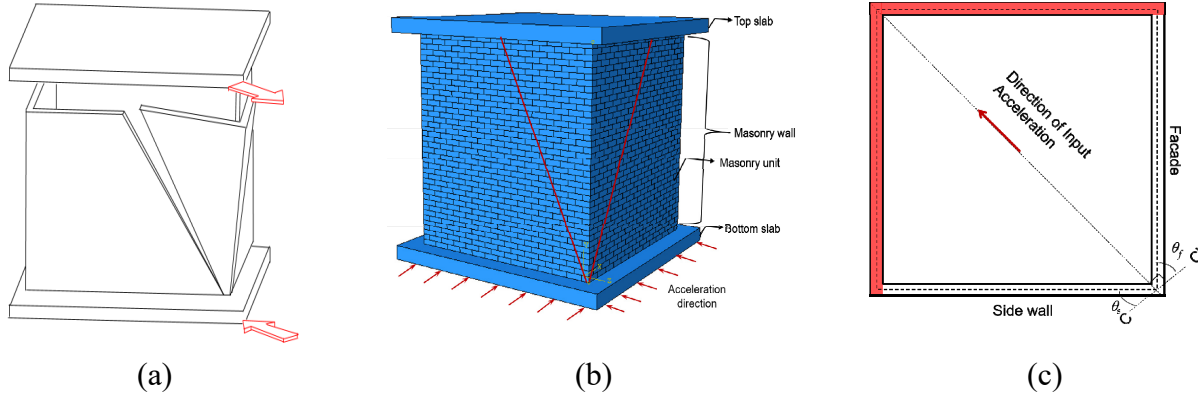


Figure 2: (a) Schematic diagram of corner failure under lateral load (b) Detail FE masonry model (c) Direction of acceleration motion in FE model

Brick element C3D8R was adopted for meshing each brick unit with a mesh size equal to $1/10^{\text{th}}$ of the largest dimension of the unit. These masonry models, shown in Figure 2(b) were made to rest over a slab. The degrees of freedom of the slab were restrained in the vertical direction and a linearly increasing horizontal accelerating motion was induced in the masonry structure through it. In order to simulate the dead load and its inertial effects, slabs having a frictional contact with the underlying brick courses were kept over the masonry walls. Both top and bottom slabs were considered to be 100 mm thick with the material modelled as homogenous, isotropic and elastic concrete. In order to solve the dynamic problem Dynamic/Explicit solver in ABAQUS was adopted.

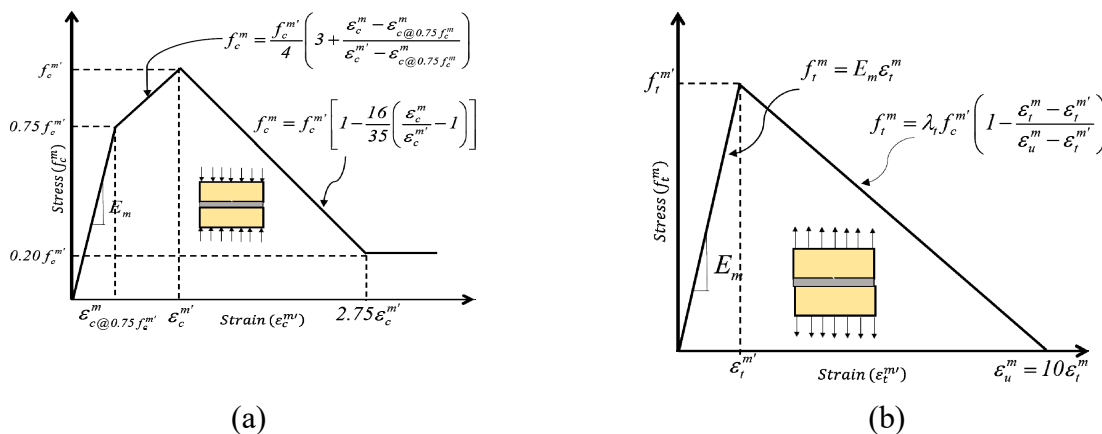


Figure 3: Stress strain curve of masonry a) Under Compression b) Under Tension

CORNER FAILURE IN DRY STACK MASONRY

In order to study the corner failure in dry stack masonry, two masonry models differing in the aspect ratio of corner walls were considered. The details of these models are summarized in

Table 1. Since the corner failure pattern may vary with the overburden pressure on walls, these models were subjected to varying levels of overburden pressure, including zero overburden i.e. non-loadbearing masonry. This overburden was applied in the form of concrete slab so that in addition to its effect under the action of gravity, the effect of inertia due to lateral accelerations can be taken into consideration.

Table 1: Details of FE models of dry masonry structures

Property	Model-1	Model-2
Sizes of the walls (mm)	1500 × 1500	2220 × 1500
	1500 × 1500	1500 × 1500
Dimensions of masonry unit (mm)	120 × 60 × 37.5	120 × 60 × 37.5
Density of masonry unit (kg/m ³)	3500	3500
Coefficient of friction	0.6	0.6
Size of slab (mm)	1800 × 1800	3120 × 2400
Thickness of Slab(mm)	100	100

Corner failure Mechanism in Non-loadbearing masonry

When non-loadbearing masonry structures were subjected to base accelerations, it was observed that a wedge shape portion detaches from the masonry walls at corners. The crack pattern leading to such failures reveals three different types of cracks. Initially, under the action of out-of-plane forces, a horizontal crack develops in the mid-section of the wall. From the ends of this horizontal crack, stepped and vertical cracks develop subsequently. The stepped crack propagates towards the lower end of the wall while the vertical crack grows towards the top edge of the wall as shown in Figures 4(a) & (b). The cracks from the two mutually orthogonal walls combine to form a failure plane and a wedge shaped portion that separates from the surrounding masonry and tends to overturn about the base as shown in Figure 4(c) & (d).

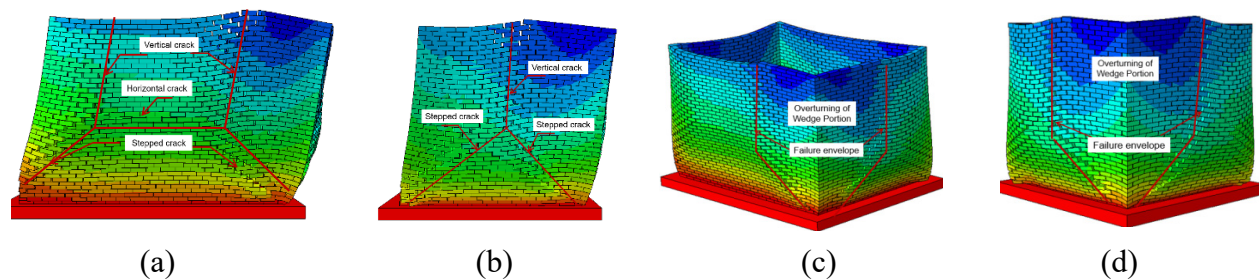


Figure 4: Corner failure in non-loadbearing masonry (a) Crack pattern in the side walls of Model-2 (b) Crack pattern in the side walls of Model-1 (c) Overturning of wedge portion in Model-2 (d) Overturning of wedge portion Model-1

On comparing the crack patterns in walls with different lengths and same height, it was observed that as the length of the wall is decreased, the length of the horizontal crack also decreases. This causes the two vertical cracks to come close and in the limiting situation, they merge to form a single vertical crack. This can be observed by comparing Figure 4 (a) & (b). Up to this limiting

case the horizontal crack is formed at a height of approximately 0.4 times the height of the wall, h . With further reduction in the length of the wall, the height at which the horizontal crack is formed is further reduced. For each type of failure pattern, the lengths of the horizontal and the vertical projections of the stepped cracks, in terms of dimensions of the brick (length, l_b and thickness, t_b) and the wall, are shown in Figure 5.

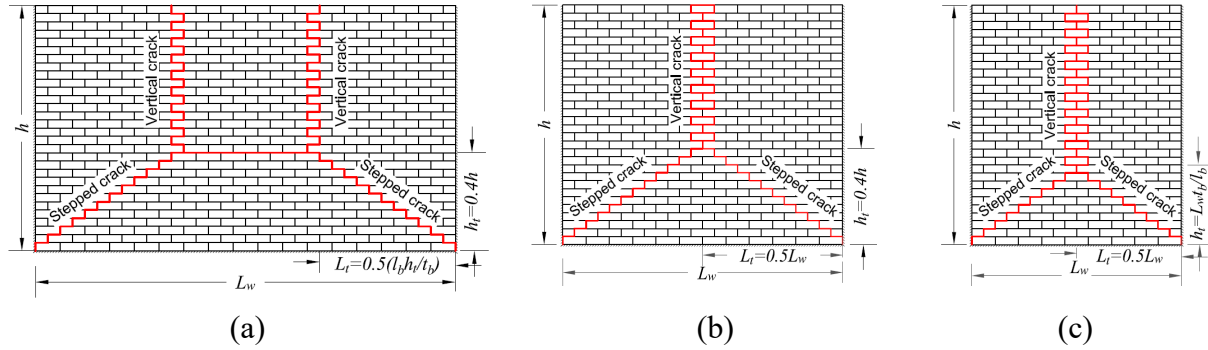


Figure 5: Out-of-plane failure pattern in walls supported on three edges (a) General failure pattern (b) Failure pattern in limiting case (c) Failure pattern beyond limiting case

Based on the failure pattern observed in FE simulations, a failure mechanism has been proposed for the corner failures in non-loadbearing masonry walls as shown in Figure 6(a). The unshaded portion represents the failure wedge which has a tendency to rotate about the axis C-C'. The two walls at the corner can be identified as the façade wall (with subscript f) and side wall (with subscript s). The dislodging portion of each wall has been sub-divided into a triangular section (comprising of the stepped crack) and a rectangular section (comprising of the vertical crack) with corresponding parameters represented by subscripts t and r respectively. For this failure mechanism, an expression for limiting acceleration, a_{lim} can be derived considering the moment equilibrium about the axis of rotation of the wedge, C-C'. The overturning moment on the failure (wedge) portion due to inertial forces is resisted by the stabilizing moment due to the weight of the side and the façade walls along with the resistance due to the interlocking friction force, C in the vertical crack.

Moment due to inertial forces about axis C-C' is given by

$$\frac{a_{lim}}{g} [W_s h_{sc} + W_f h_{fc}] \quad (1)$$

The resisting moment due to the weight of dislodging wedge about C-C' is given by

$$W_s l_{sc} \cos(\theta_f) + W_f l_{fc} \cos(\theta_s) \quad (2)$$

Based on Figure 6(b), the shear resistance offered by the n (equal to h_r/t_b) number of interlocked bricks each of weight W_b and friction coefficient μ , is given by

$$C = \mu \frac{n(n+1)}{2} \frac{W_b}{2} \quad (3)$$

Therefore, total resisting moment due to interlocking in side and façade walls about C-C' is given by

$$C_s h_{isc} + C_f h_{ffc} \quad (4)$$

Equating the total resisting moment as sum of Eq. (2) and Eq. (4) to the de-stabilizing moment due to inertial forces about the axis of rotation, C-C', the limiting acceleration can be obtained as follows:

$$a_{lim} = \frac{C_s h_{isc} + W_s l_{sc} \cos(\theta_f) + C_f h_{ffc} + W_f l_{fc} \cos(\theta_s)}{W_s h_{sc} + W_f h_{fc}} g \quad (5)$$

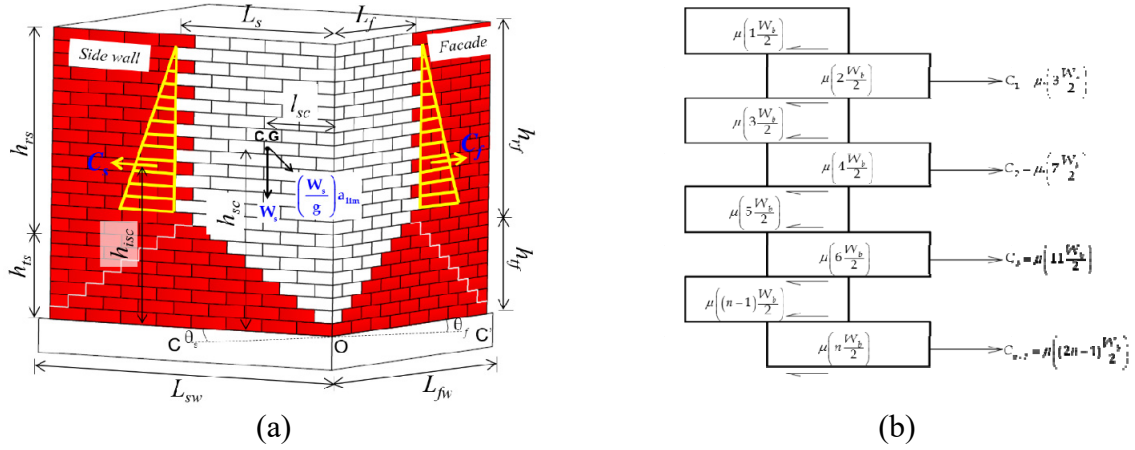


**Figure 6: (a) Corner failure mechanism in Non-Loadbearing masonry structure
(b) Frictional force at brick interface in the interlocking section**

Corner failure mechanism in loadbearing masonry

In case of load bearing masonry, the observed corner failure pattern in FE simulations was primarily due to sliding of the bricks in the plane of the wall. This indicates that in-plane (IP) component of the lateral force is primarily responsible for failure in such type of masonry. The observed crack pattern comprises of stepped cracks originating from the diagonal ends and an ‘intersecting’ crack combining these stepped cracks to form the single crack as shown in Figure 7(a). The sequence of formation of such a crack pattern can be explained as follows: Initially due to the shear force developed on top of the wall by inertial forces in the slab, the brick courses directly beneath begin to slide forming the stepped crack. Due to this sliding, high compressive stress builds up over the mid portion of the wall as it directly supports the displaced brick courses. The resulting high compressive stress prevents bricks in the mid portion of the wall from relative sliding because of which the crack in this section remains nearly vertical. This vertical crack will continue up to the point where it meets that stepped crack which terminates at the toe. The stepped crack in the lower portion offers least resistance to overturning. As the length of the wall is increased with respect to its height, the length of the stepped crack increases leading to a reduction in the length of the intersecting crack as shown in Figure 7(b). Cracks from both the corner walls unite to form a failure plane, thereby leading to separation and overturning of the wedge portion about its toe as shown in Figure 7(c) and (d).

Based on the failure pattern in loadbearing masonry, the overall failure pattern can be represented by Figure 8(a). On closely observing the intersecting crack, it can be seen that it comprises of certain interlocked bricks (sub-interlocking) which are joined by smaller stepped cracks. For limit analysis, these different sub-interlocks have been combined to form a single interlocked cracked section resulting in a failure mechanism as shown in Figure 8(b).

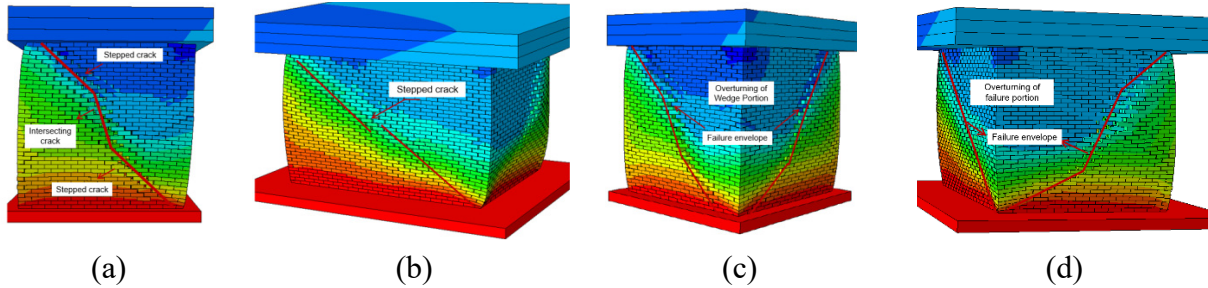


Figure 7: Corner failure in load bearing masonry (a) Crack pattern in side wall of Model-1 (b) Crack pattern in shorter wall of Model-2 (c) Overturning of wedge portion in Model-1 (d) Overturning of failure portion in Model-1

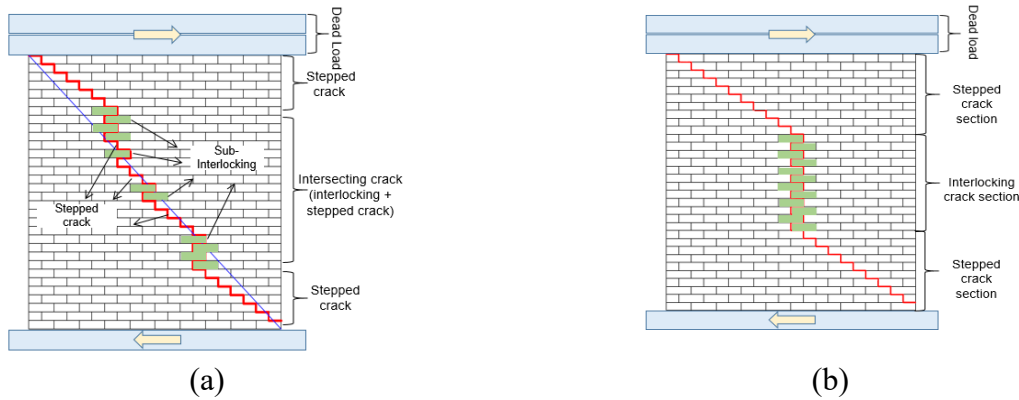


Figure 8: In-plane crack pattern (a) Observed crack pattern (b) Idealized crack pattern

Based on the above observations, a schematic for the corner failure mechanism for loadbearing walls is shown in Figure 9(a). The unshaded portion of masonry walls represents the failure wedge. A value of the limiting acceleration, a_{lim} , can be obtained by considering moment equilibrium about C-C' as discussed above. In addition to moment due to various forces discussed for non-loadbearing walls, it will include the effect of dead load, w_d over the masonry. Since in this case interlocking lies at the mid-section of the wall, the total shear resistance, C will include the effect of the weight of the trapezoidal section as well as the dead load lying directly above the interlocked section. The overall equation for shear resistance for loadbearing walls is given by,

$$C = \mu \frac{n(n+1)}{2} \frac{W_b}{2} + \mu n \frac{h_{tr}}{t_b} \frac{W_b}{2} + \mu n w_d \frac{l_b}{2} \quad (6)$$

The detaching portion of each of the orthogonal walls can be divided into a triangular, a rectangular and a trapezoidal section and parameters related to these sections are represented by

subscripts t , r and tr , respectively. In Figure 9(a), variables with subscript s and f define parameters related to side walls and façade walls respectively. Based on this failure mechanism, the limiting acceleration for loadbearing walls is given by,

$$a_{lim} = \frac{C_s h_{isc} + \left[W_s l_{sc} + w_{ds} \frac{L_s^2}{2} \right] \cos(\theta_f) + C_f h_{ifc} + \left[W_f l_{fc} + w_{df} \frac{L_f^2}{2} \right] \cos(\theta_s)}{\left[W_s h_{sc} + w_{ds} L_s h \right] + \left[W_f h_{fc} + w_{df} L_f h \right]} g \quad (7)$$

As discussed earlier, with increase in the length of the wall, the length of the intersecting crack decreases. This situation will continue until its length reduces to zero. Thereafter, the stepped cracks will be joined by a horizontal crack as shown in Figure 9(b). Mathematically, let α_b be the angle of stepped crack and α_p be the angle of wall panel. Then, if α_b is greater than α_p , there will interlocking. Else, there will be no interlocking. Similar equations can be derived for a loadbearing masonry assemblage with no interlocking.

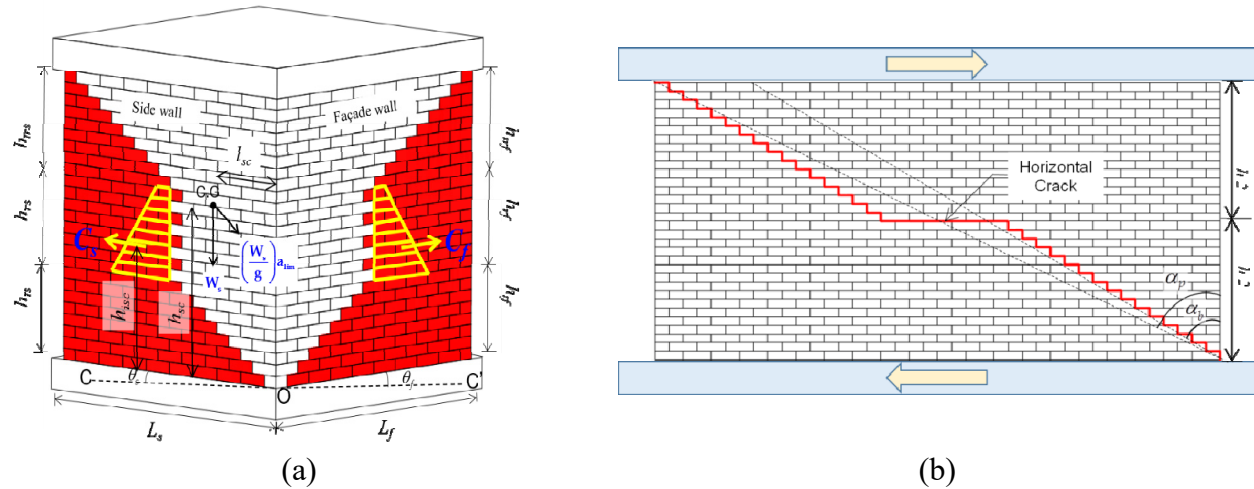


Figure 9: (a) Corner failure mechanism in loadbearing masonry structure (b) Failure mechanism in wall with no interlocking

Limit analysis versus FE prediction

The values of limiting accelerations obtained from the limit analysis for the idealized failure mechanisms were further verified by a dynamic analysis in which the FE model was subjected to a pulse load at the base. The response was examined after a time equal to $0.5T_n$, when the maximum dynamic response of an elastic single-degree-of-freedom structure for a rectangular pulse loading occurs, where T_n is natural period of the structure. Unreinforced masonry structures typically have fundamental natural periods lying in the range of 0.25s to 0.4s which can be higher for dry masonry structures as they are more deformable and flexible. Therefore, for dry masonry structures, it can be assumed that the fundamental natural periods would be in the range of 0.5s to 1s and thus the maximum response of such structures under pulse loading is expected to occur between 0.25s to 0.5s of the loading. When FE models of the masonry structures were subjected to pulse loading with base acceleration equal to the limiting

acceleration obtained from limit state analysis, the wedge portions were observed to detach from the surrounding masonry within the above-mentioned time. Table 2 shows the limiting accelerations, obtained from Eqs. 5 & 7, which were applied to the masonry models as pulse loadings.

Table 2: Limiting acceleration for various dry masonry models

Load Case	Model	Overburden Pressure(kPa)	Limiting Acceleration (g)
1	Model-1	0	1.16
2	Model-2	0	1.03
3	Model-1	22	0.56
4	Model-2	183(Long wall), 148(Short wall)	0.54

CORNER FAILURES IN MORTAR BONDED MASONRY

Often in mortar bonded masonry, the behaviour of mortar is simulated by introducing the cohesive elements between brick courses. However such an approach is not only computationally intensive but also difficult to formulate. Therefore, in this study, a new strategy of modelling this type of masonry has been proposed wherein, instead of cohesive elements, friction is introduced between the brick surfaces so as to simulate the behaviour of mortar in shear. Brick-mortar interface obeys the Mohr-Coulomb law. So shear resistance offered by mortar is given by

$$\tau = \tau_o + \sigma_c \mu \quad (8)$$

where, τ_o is the shear resistance at zero pre-compression, and σ_c is pre-compressive stress due to load over any given masonry course level [9]. In order to introduce the shear resistance calculated from Eq. 8, a new term '*equivalent coefficient of friction*', μ_{eq} has been introduced. It is the coefficient of friction which when multiplied by the vertical pre-compressive stress resists the shear of same magnitude as resisted by the mortar at any masonry course level. Mathematically, for any n^{th} course Eq. 8 can be modified as follows,

$$\left(\mu_{eq}\right)_n = \frac{\tau_o}{\left(\sigma_c\right)_n} + \mu \quad (9)$$

Eq. (9) implies that with increase in overburden over the masonry, the value of equivalent friction coefficient tends to become same for all the courses. This situation is similar to dry masonry in which all courses have the same value of friction coefficient. Therefore, for masonry with high overburden pressure, failure pattern should be similar to that of dry masonry.

For studying the corner failures in mortar-bonded masonry, Model-1 considered for dry masonry was modified by introducing the equivalent coefficient of friction at each interface of the brick courses. In order to observe the variation in the failure pattern of masonry with increasing overburden, the masonry model was loaded with 1 and 5 slabs, i.e., pre-compression of 22 kPa and 110 kPa, respectively. When the masonry model with pre-compression of 22 kPa was subjected to linearly accelerating motion along the corner, sudden opening of the cracks through

brick bed joints was observed as shown in Figure 10(a). In case of masonry model with pre-compression of 110 kPa, the observed cracks were mainly due to sliding of the bricks, similar to that observed in dry masonry, as shown in Figure 10(b). This validates the assertion that mortar bonded masonry behaves like dry masonry under heavy dead load conditions.

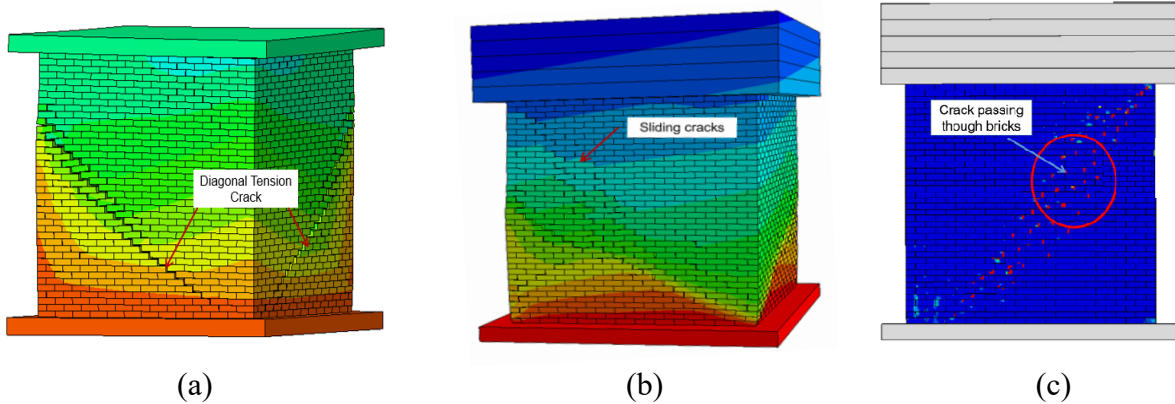


Figure 10: Crack pattern for load bearing masonry (a) Diagonal tension crack in model with Pre-compression of 22 kPa (b) Sliding cracks in model with Pre-compression of 110 kPa (c) Crack passing through brick in model with pre-compression of 110 kPa

Moreover, along the path of sliding cracks, local tensile cracks were observed passing through the bricks as shown in Figure 10(c). This may be because of the high shear resistance at brick interfaces which prevents a complete sliding out of the interlocked bricks leading to cracking either due to bending or due to axial tension. Also, when the failure portion of a heavily loaded wall tends to rotate about its toe, the self-weight of failure portion as well as the dead load over it is transferred to the ground through the toe. Thus, the toe is subjected to a rather concentrated load which leads to a crushing failure as shown in Figure 11(a). Such toe crushing is also observed in earthquake damaged structures as shown in Figure 11(b).

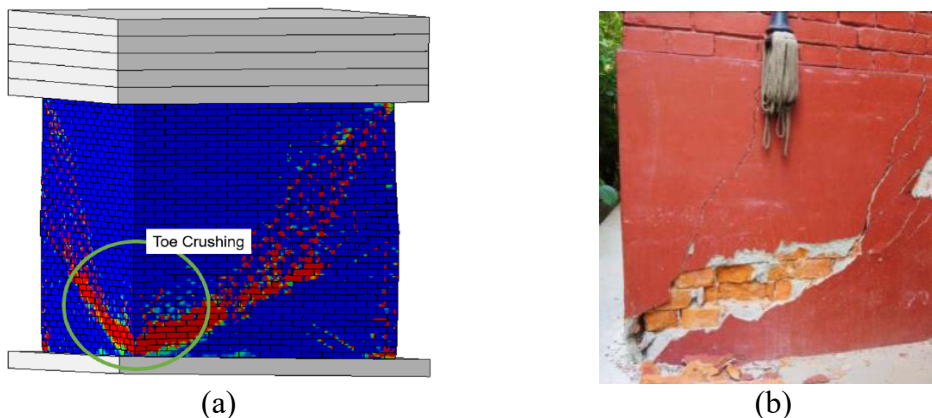


Figure 11: Toe crushing of corner walls (a) Model with pre-compression of 6.75 kN/m (110 kPa) (b) Observed failure in the 2015 Nepal Earthquake [10]

CONCLUSIONS

Corner failure of masonry structures was studied using FE technique in which masonry models were subjected to linearly increasing accelerating motion acting diagonally along the corner. In case of dry stack masonry, distinct failure patterns were obtained for non-loadbearing and loadbearing masonry. Failure pattern for the case of non-loadbearing walls was found to be due to the out-of-plane component while that for loadbearing walls was due to the in-plane component of the lateral load. Based on these observed failure patterns, failure mechanisms were proposed and limiting acceleration values were obtained. These limiting acceleration values compared well with finite element predictions. A new approach was adopted to simplify the micro-modelling of mortar bonded masonry by introducing an *equivalent coefficient of friction*. This approach was found to be effective in determining the propagation of crack through the masonry as well as the value of acceleration at which a portion of corner walls detaches from the surrounding masonry.

REFERENCES

- [1] Tampone G. (1999). "Tipologie degli edifici danneggiati dal sisma." *Manuale per la riabilitazione e la ricostruzione postsismica degli edifici (1999)*. Regione dell'Umbria. Dei ed ["Types of buildings damaged by the earthquake". *Handbook for rehabilitation and post-earthquake reconstruction of buildings (1999)*. Umbria region, Italy
- [2] International rescue corps (2001). Retrieved May 2016, from <http://www.intrescue.info/hub/index.php/missions/indian-earthquake-jan-2001>
- [3] The Australian (2012). Retrieved July 2016, from <http://www.theaustralian.com.au/news/world/historic-buildings-factories-reduced-to-rubble-after-quake-hits-italys-northeast/story-e6frg6so-1226361851705>
- [4] D'Ayala, D., and Speranza, E. (2003). "Definition of Collapse mechanisms and seismic vulnerability of historic masonry buildings". *Earthquake Spectra*, 19, 479-509.
- [5] Kaushik H.B., Rai D.C. and Jain S.K. (2007). "Uniaxial compressive stress-strain model for clay brick masonry". *Current Science*, 92(4), 497-501
- [6] Akhaveissy, A.H. and Desai, C.S. (2011). "Unreinforced Masonry Walls: Nonlinear Finite Element Analysis with a Unified Constitutive Model." *Archives of Computational Methods in Engineering*, 18(4), 485-502
- [7] Mills, R.S., Krawinkler, H., and Gere, J.M. (1979). "Model tests on earthquake simulators-development and implementation of experimental procedures." *Report No. 39*, John A. Blume Earthquake Engineering Research Institute (EERI), CA, USA.
- [8] Tassios, T.P. (1992). "Modelling of structures subjected to seismic loading." *Small Scale Modelling of Concrete Structures*, F.A. Noor and L.F. Boswell, eds., Elsevier Applied Science, New York, 229-271
- [9] Hendry, A., and Sinha, B. (1997). *Design of masonry structures*, E & FN Spon, London
- [10] Dizhur, D. (2016). "Building typologies and failure modes observed in the 2015 Gorkha (Nepal) Earthquake". *Bulletin of the New Zealand Society for Earthquake Engineering*, 49, 211-232.